

RESEARCH

Open Access



# Fe<sub>3</sub>O<sub>4</sub>@SiO<sub>2</sub>-SnCl<sub>4</sub>-promoted synthesis, cytotoxic evaluation, molecular docking, and MD simulation of some indenopyrido[2,3-*d*] pyrimidine derivatives

Leila Emami<sup>1</sup>, Ladan Baziyar<sup>2</sup>, Al-Anood Mohammad Al-Dies<sup>3</sup>, Sara Sadeghian<sup>2</sup>, Bi Bi Fatemeh Mirjalili<sup>4</sup>, Zeinab Faghih<sup>1</sup>, Sajad Khorasani<sup>1</sup>, Leila Zamani<sup>1</sup> and Soghra Khabnadideh<sup>1,2\*</sup>

## Abstract

In this study, an efficient and environmentally friendly method for the one-pot synthesis of indenopyrido[2,3-*d*] pyrimidine derivatives was developed using Fe<sub>3</sub>O<sub>4</sub>@SiO<sub>2</sub>-SnCl<sub>4</sub> nanoparticles as a catalyst. Indenopyrido[2,3-*d*] pyrimidines (**4a-4j**) were synthesized via three-component couplings of 6-amino-2-(methylthio)pyrimidin-4(3*H*)-one, 1,3-indanedione, and aldehydes in water as the solvent. In this reaction, Fe<sub>3</sub>O<sub>4</sub>@SiO<sub>2</sub>-SnCl<sub>4</sub> demonstrated a highly catalytic nature, an easy handling procedure, short reaction times, recyclability exploitation, and excellent yields. The cytotoxic activities of the synthesized indenopyrido[2,3-*d*] pyrimidines analogues were evaluated against three cancer cell lines; MCF-7 (breast carcinoma), A549 (lung non-small cell carcinoma), and SKOV3 (ovarian carcinoma) using MTT assay. Additionally, molecular docking studies and molecular dynamics (MD) simulation of the investigated compounds was performed to verify their binding modes toward EGFR kinase receptor as the possible targets. This analysis aimed to predict the antitumor mechanisms of the synthesized compounds. The binding free energy values of the compounds showed a satisfactory correlation with their cytotoxic activities.

**Keywords** Indenopyrido[2,3-*d*]pyrimidine, Cytotoxic activity, Molecular docking, MD Simulation

## Introduction

Cancer is a disease characterized by abnormal cell proliferation and the invasion of healthy tissues. Cancer is caused by a combination of environmental factors and genetic disorders. Chemotherapy, often combined

with surgery, is typically the most effective anticancer treatment; however, the effectiveness of chemotherapy can be limited by drug resistance and toxicity [1]. Combination therapy targeting multiple molecular pathways uniquely expressed in tumor cells holds promise for the development of more selective anticancer drugs with reduced toxicity and side effects [2, 3].

Pyrido[2,3-*d*]pyrimidines are nitrogen-containing heterobicyclic compounds with various pharmaceutical applications, such as antimicrobial [4–7], antiallergic [8], antitumor [9, 10], antileishmania [11], antiviral [12], antihypertensive [13], antianalgesic, anti-inflammatory [14], anticancer, and inhibition of dihydrofolate reductase or tyrosine kinase [15–17]. Furthermore, indenopyrimidines and their derivatives

\*Correspondence:

Soghra Khabnadideh  
khabns@sums.ac.ir

<sup>1</sup> Pharmaceutical Sciences Research Center, Faculty of Pharmacy, Shiraz University of Medical Sciences, Shiraz, Iran

<sup>2</sup> Department of Medicinal Chemistry, Faculty of Pharmacy, Shiraz University of Medical Sciences, P.O. Box: 71345-1798, Shiraz, Iran

<sup>3</sup> Department of Chemistry, Al Qunfudah University College, UMM Al-Qura University, Mecca, Saudi Arabia

<sup>4</sup> Department of Chemistry, College of Science, Yazd University, Yazd, Iran



© The Author(s) 2025. **Open Access** This article is licensed under a Creative Commons Attribution-NonCommercial-NoDerivatives 4.0 International License, which permits any non-commercial use, sharing, distribution and reproduction in any medium or format, as long as you give appropriate credit to the original author(s) and the source, provide a link to the Creative Commons licence, and indicate if you modified the licensed material. You do not have permission under this licence to share adapted material derived from this article or parts of it. The images or other third party material in this article are included in the article's Creative Commons licence, unless indicated otherwise in a credit line to the material. If material is not included in the article's Creative Commons licence and your intended use is not permitted by statutory regulation or exceeds the permitted use, you will need to obtain permission directly from the copyright holder. To view a copy of this licence, visit <http://creativecommons.org/licenses/by-nc-nd/4.0/>.

have demonstrated various pharmacological activities, particularly anticancer activity [18–23].

Consequently, this class of compounds has attracted significant research attention. Several multicomponent reaction (MCR) methods have been reported for the synthesis of pyrido[2,3-*d*]pyrimidines [24–30]. Various methods have been developed for the synthesis of pyrido[2,3-*d*]pyrimidines through three-component condensation reaction involving aldehydes, 1,3-dicarbonyl compounds, and 6-aminopyrimidine-2,4-dione. These reactions are facilitated by different catalysts, including [bmim]Br, *P*-TSA, InCl<sub>3</sub>, nano-Fe<sub>3</sub>O<sub>4</sub>@SiO<sub>2</sub>-SO<sub>3</sub>H, Fe<sub>3</sub>O<sub>4</sub> nanoparticles supported on cellulose (Fe<sub>3</sub>O<sub>4</sub>NPs-Cell), RuCl<sub>3</sub>.xH<sub>2</sub>O, and TEDA/IMIZBAIL@ UiO-66 [31, 32]. Although most of these methods offer distinct advantages, some of the reported methods have drawbacks, including prolonged reaction times, low product yields, high temperatures, need for organic solvents, and the requirement for highly corrosive catalysts [31–33].

In some cases, the used catalysts are harmful to the environment and cannot be reused. Therefore, an efficient method for the preparation of pyrido[2,3-*d*]pyrimidine derivatives is still desirable. In this work, we report an efficient and eco-friendly procedure for the preparation of indenopyrido[2,3-*d*]pyrimidine in the presence of Fe<sub>3</sub>O<sub>4</sub>@SiO<sub>2</sub>-SnCl<sub>4</sub> [34–36]. Additionally, some of the synthesized compounds were evaluated for their antitumor activity.

In recent years, a number of indeno [1, 2-*d*] pyrimidine and pyrido[2,3-*d*]pyrimidines derivatives have been reported as anticancer agents. For example, an indeno [1, 2-*d*] pyrimidine derivative (**I**) has been reported as anti-breast cancer agent [1]. Also, a large number of pyrido[2,3-*d*]pyrimidine derivatives (**II** and **III**) have shown significant anticancer activity [2, 3] (Fig. 1).

In the present work, an efficient and environmentally friendly method for the one-pot synthesis of

indenopyrido[2,3-*d*]pyrimidine derivatives was developed using Fe<sub>3</sub>O<sub>4</sub>@SiO<sub>2</sub>-SnCl<sub>4</sub> nanoparticles as a catalyst. Then, the in vitro cytotoxic activities of ten indenopyrido[2,3-*d*]pyrimidine derivatives (**4a–j**), which contain different substituted phenyl rings at position 4 of the pyridopyrimidine system, were evaluated using an in vitro MTT assay on three human cancer cell lines, MCF-7 (breast carcinoma), A549 (lung non-small cell carcinoma), and SKOV3 (ovarian carcinoma). Additionally, molecular docking studies and molecular dynamics (MD) simulation were performed to explore the most appropriate orientation and binding modes of examined compounds towards the EGFR as possible target.

## Results and discussion

### Chemistry

Following our studies on the development of benign methods for the synthesis of biologically important heterocycles [37–41], we utilized the valuable magnetic nanoparticles catalyst Fe<sub>3</sub>O<sub>4</sub>@SiO<sub>2</sub>-SnCl<sub>4</sub> [34, 35, 42–44]. A simple one-pot three-component reaction involving 6-amino-2(methylthio)pyrimidin-4(3H)-one (**1**), 1,3-indanedione (**2**), and various aryl aldehydes (**3**), was conducted in the presence of the nanocatalyst, Fe<sub>3</sub>O<sub>4</sub>@SiO<sub>2</sub>-SnCl<sub>4</sub> under reflux and ultrasound irradiation in water. This approach successfully yielded the corresponding indenopyrido[2,3-*d*]pyrimidines (**4a–4j**) (Fig. 2).

To optimize the desired reaction conditions, the preparation of 5-(4-chlorophenyl)-2-(methylthio)-3H-indeno[2',1':5,6]pyrido[2,3-*d*]pyrimidine-4,6-(5H,11H)-dione (**4 g**) was selected as the model reaction. In initial experiments, the effects of solvents and reaction temperature were evaluated for this model reaction in the presence of Fe<sub>3</sub>O<sub>4</sub>@SiO<sub>2</sub>-SnCl<sub>4</sub>, and results are summarized in Table 1. It is evident from the results that using Fe<sub>3</sub>O<sub>4</sub>@SiO<sub>2</sub>-SnCl<sub>4</sub> as a catalyst in water at 70 °C is the most

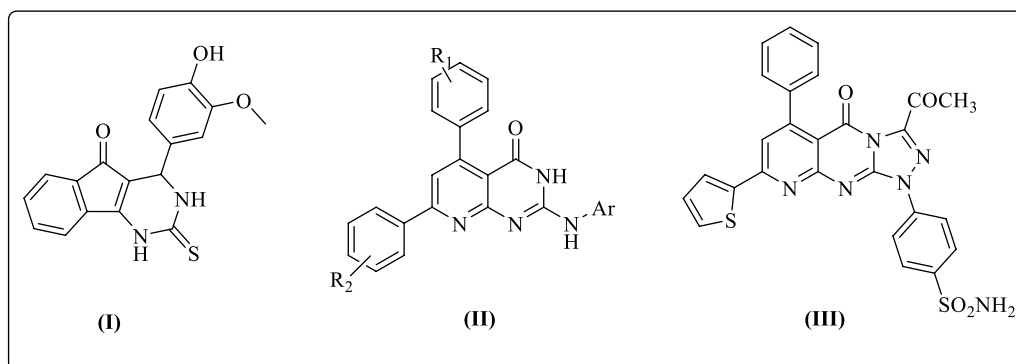


**Fig. 1** Indeno [1, 2-*d*] pyrimidine and pyrido[2,3-*d*]pyrimidines derivatives with anticancer activity

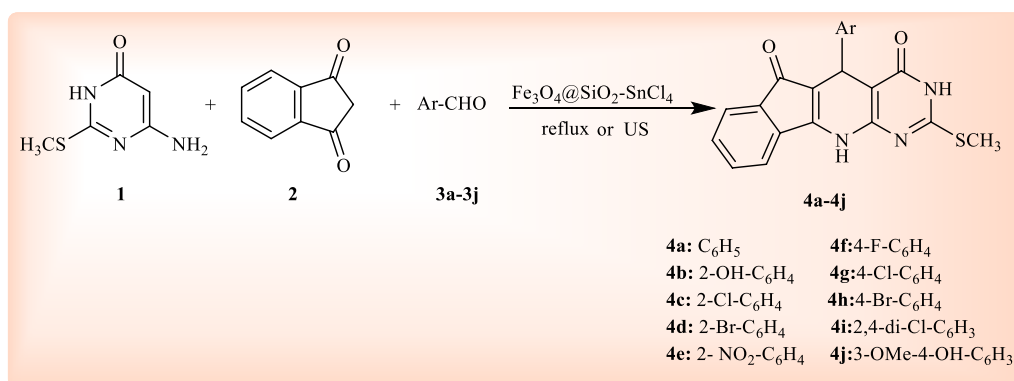


**Fig. 2** Synthesis of indenopyrido[2,3-d]pyrimidines (**4a–4j**)

**Table 1** Optimization of the model reaction condition using various solvents under reflux or ultrasound irradiation<sup>a</sup>

Entry	Solvent	T (°C)	Method I (Δ) Time (min)	Yield (%) <sup>a</sup>	Method II (US) Time (min)	Yield (%) <sup>b</sup>
1	H <sub>2</sub> O	rt	70	60	12	70
2	H <sub>2</sub> O	50	60	75	7	85
3	H <sub>2</sub> O	60	50	80	5	90
4	H <sub>2</sub> O	70	40	85	4	90
5	H <sub>2</sub> O	80	40	85	4	90
6	EtOH	70	70	75	7	82
7	MeOH	60	80	60	8	70
8	Acetone	50	70	50	10	60
9	CH <sub>3</sub> CN	80	90	40	12	50
10	DMF	120	50	70	6	80
11	HOAc	110	60	70	7	75
12	Solvent-free	120	60	80	6	85

<sup>a</sup> 4-Cl benzaldehyde (1 mmol), 1,3-indanedione (1 mmol), 6-amino-2-(alkylthio)pyrimidin-4(3H)-one (1 mmol) in water (8 mL) and Fe<sub>3</sub>O<sub>4</sub>@SiO<sub>2</sub>-SnCl<sub>4</sub> (0.01 g)

<sup>b</sup> Isolated yields

effective condition, producing a higher yield (90%) in a shorter reaction time (4 min) (Table 1, Entry 4).

Considering that the amount of catalyst plays a crucial role in this reaction, the amount of required catalyst for the model reaction under the best obtained reaction conditions was optimized (Table 2). According to the results, in the absence of catalyst, no significant product was obtained. In contrast, the presence of Fe<sub>3</sub>O<sub>4</sub>@SiO<sub>2</sub>-SnCl<sub>4</sub>, led to the high yields in the reaction. For example, the synthesis of compound **4 g** as a model under ultrasound irradiation, using 0.01 g Fe<sub>3</sub>O<sub>4</sub>@SiO<sub>2</sub>-SnCl<sub>4</sub> per 1 mmol of substrate, produced **4 g** with a yield of 90% in H<sub>2</sub>O at 70 °C after 4 min. Increasing the amount of the catalyst to 0.02 g and 0.03 g resulted in yields of 94% and 98%, respectively, after 3 and 2 min. Therefore, the best result was obtained using 0.03 g Fe<sub>3</sub>O<sub>4</sub>@SiO<sub>2</sub>-SnCl<sub>4</sub> and 1 mmol

of substrate. Notably, increasing the amount of catalyst under reflux and ultrasound irradiation conditions did not lead to any significant changes in yield and reaction time (Entry 9, Table 2).

It is clear from Table 2 that Fe<sub>3</sub>O<sub>4</sub>@SiO<sub>2</sub>-SnCl<sub>4</sub> has proven to be the more efficient catalyst for the synthesis of desired products. The model reaction was performed using nano-Fe<sub>3</sub>O<sub>4</sub>, SnCl<sub>4</sub>-SiO<sub>2</sub> and Fe<sub>3</sub>O<sub>4</sub>@SiO<sub>2</sub> (Table 2, Entries 2,3 and 4). As shown in Table 2, the Fe<sub>3</sub>O<sub>4</sub>@SiO<sub>2</sub>-SnCl<sub>4</sub> act as a suitable catalyst in terms of yields. The proficient catalytic activity of Fe<sub>3</sub>O<sub>4</sub>@SiO<sub>2</sub>-SnCl<sub>4</sub> was related to the -SnCl<sub>4</sub> groups of the catalyst, which provide efficient acidic sites.

Using the described optimal conditions, several derivatives of indenopyrido[2,3-d]pyrimidines (**4a–4j**) were prepared in high yields (94–99%) and within short reaction times (1.5–3 min) (Table 3). No significant effect of

**Table 2** Optimization of the model reaction using Fe<sub>3</sub>O<sub>4</sub>@SiO<sub>2</sub>-SnCl<sub>4</sub> under reflux (I) and ultrasound irradiation (II) in water<sup>a</sup>

Entry	Method I (Δ)		Method II (US)	
	Catalyst/(g)		Catalyst/(g)	
	Time (min)	Yield (%) <sup>b</sup>	Time (min)	Yield (%) <sup>b</sup>
1	none		none	
	120	35	20	40
2	Fe <sub>3</sub> O <sub>4</sub> @SiO <sub>2</sub> /0.10		Fe <sub>3</sub> O <sub>4</sub> @SiO <sub>2</sub> /0.10	
	30	55	10	60
3	nano-Fe <sub>3</sub> O <sub>4</sub> /0.10		nano-Fe <sub>3</sub> O <sub>4</sub> /0.10	
	30	70	10	75
4	SnCl <sub>4</sub> /SiO <sub>2</sub> /0.10		SnCl <sub>4</sub> /SiO <sub>2</sub> /0.10	
	50	60	12	70
5	Fe <sub>3</sub> O <sub>4</sub> @SiO <sub>2</sub> -SnCl <sub>4</sub> /0.005		Fe <sub>3</sub> O <sub>4</sub> @SiO <sub>2</sub> -SnCl <sub>4</sub> /0.005	
	45	75	7	80
6	Fe <sub>3</sub> O <sub>4</sub> @SiO <sub>2</sub> -SnCl <sub>4</sub> /0.010		Fe <sub>3</sub> O <sub>4</sub> @SiO <sub>2</sub> -SnCl <sub>4</sub> /0.010	
	40	85	4	90
7	Fe <sub>3</sub> O <sub>4</sub> @SiO <sub>2</sub> -SnCl <sub>4</sub> /0.020		Fe <sub>3</sub> O <sub>4</sub> @SiO <sub>2</sub> -SnCl <sub>4</sub> /0.020	
	30	85	3	94
8	Fe <sub>3</sub> O <sub>4</sub> @SiO <sub>2</sub> -SnCl <sub>4</sub> /0.030		Fe <sub>3</sub> O <sub>4</sub> @SiO <sub>2</sub> -SnCl <sub>4</sub> /0.030	
	20	88	2	98
9	Fe <sub>3</sub> O <sub>4</sub> @SiO <sub>2</sub> -SnCl <sub>4</sub> /0.040		Fe <sub>3</sub> O <sub>4</sub> @SiO <sub>2</sub> -SnCl <sub>4</sub> /0.040	
	20	88	2	98

<sup>a</sup> 4-Cl-benzaldehyde (1 mmol), 1,3-indanedione (1 mmol), 6-amino-2-(alkylthio)pyrimidin-4(3H)-one (1 mmol) in water (8 mL) at 70 °C

<sup>b</sup> Isolated yields

**Table 3** Synthesis of indenopyrido[2,3-d]pyrimidine derivatives under reflux conditions (method I) and sonication (method II) (Fig. 3)<sup>a</sup>

Product	Ar	Time (min)/Yield (%) <sup>b</sup>	
		Method I (Δ)	Method II (US)
4a	C <sub>6</sub> H <sub>5</sub>	30/80	3/94
4b	2-OH-C <sub>6</sub> H <sub>4</sub>	28/84	2.5/95
4c	2-Cl-C <sub>6</sub> H <sub>4</sub>	24/89	2/97
4d	2-Br-C <sub>6</sub> H <sub>4</sub>	24/88	2/97
4e	2-NO <sub>2</sub> -C <sub>6</sub> H <sub>4</sub>	24/88	2/96
4f	4-F-C <sub>6</sub> H <sub>4</sub>	18/90	1.50/99
4g	4-Cl-C <sub>6</sub> H <sub>4</sub>	20/88	2/98
4h	4-Br-C <sub>6</sub> H <sub>4</sub>	20/86	2/98
4i	2,4-di-Cl-C <sub>6</sub> H <sub>3</sub>	20/89	2/98
4j	3-OMe-4-OH-C <sub>6</sub> H <sub>3</sub>	27/86	2.5/97

<sup>a</sup> arylaldehyde (1 mmol), 1,3-indanedione (1 mmol), 6-amino-2-(alkylthio)pyrimidin-4(3H)-one (1 mmol) in water (8 mL) and Fe<sub>3</sub>O<sub>4</sub>@SiO<sub>2</sub>-SnCl<sub>4</sub>(0.01 g) at 70 °C

<sup>b</sup> Isolated yields

the electronic nature of substituents in the aromatic aldehydes ring was observed. Both aromatic aldehydes containing electron-donating groups (such as methoxy and methyl group) and electron-withdrawing groups (such

as halides and nitro group) were utilized, resulting in the corresponding products (**4a–4j**) in high yields under the optimized reaction conditions. The structures of all products were confirmed by spectroscopic methods (IR, <sup>1</sup>H NMR and <sup>13</sup>C NMR).

A proposed mechanism for the synthesis of indenopyrido[2,3-d]pyrimidines in the presence of Fe<sub>3</sub>O<sub>4</sub>@SiO<sub>2</sub>-SnCl<sub>4</sub> as a Lewis acid catalyst, is shown in Fig. 3.

The carbonyl oxygen of aldehyde coordinates with the Lewis acid moiety, increasing the electrophilicity of the carbonyl group and enabling the reaction to be carried out in a short time. In a plausible mechanism, it is assumed that the reaction initially proceeds through the Knoevenagel condensation between arylaldehydes and 1,3-indanedione to form intermediate (I). Next, the Michael addition of 6-amino-2-(methylthio)-pyrimidin-4(3H)-one to intermediate (I) affords (II). Intermediate (II) converts to (III) after tautomerization. Then, intermediate (III) converts to (IV) via cyclization. Finally, the desired product (V) is obtained after the tautomerization of (IV) (Fig. 3).

Consequently, it is essential for the solid acid to maintain strong acidity even after recycling, which is one of the most important benefits for commercial applications. The catalyst was also recycled and reused

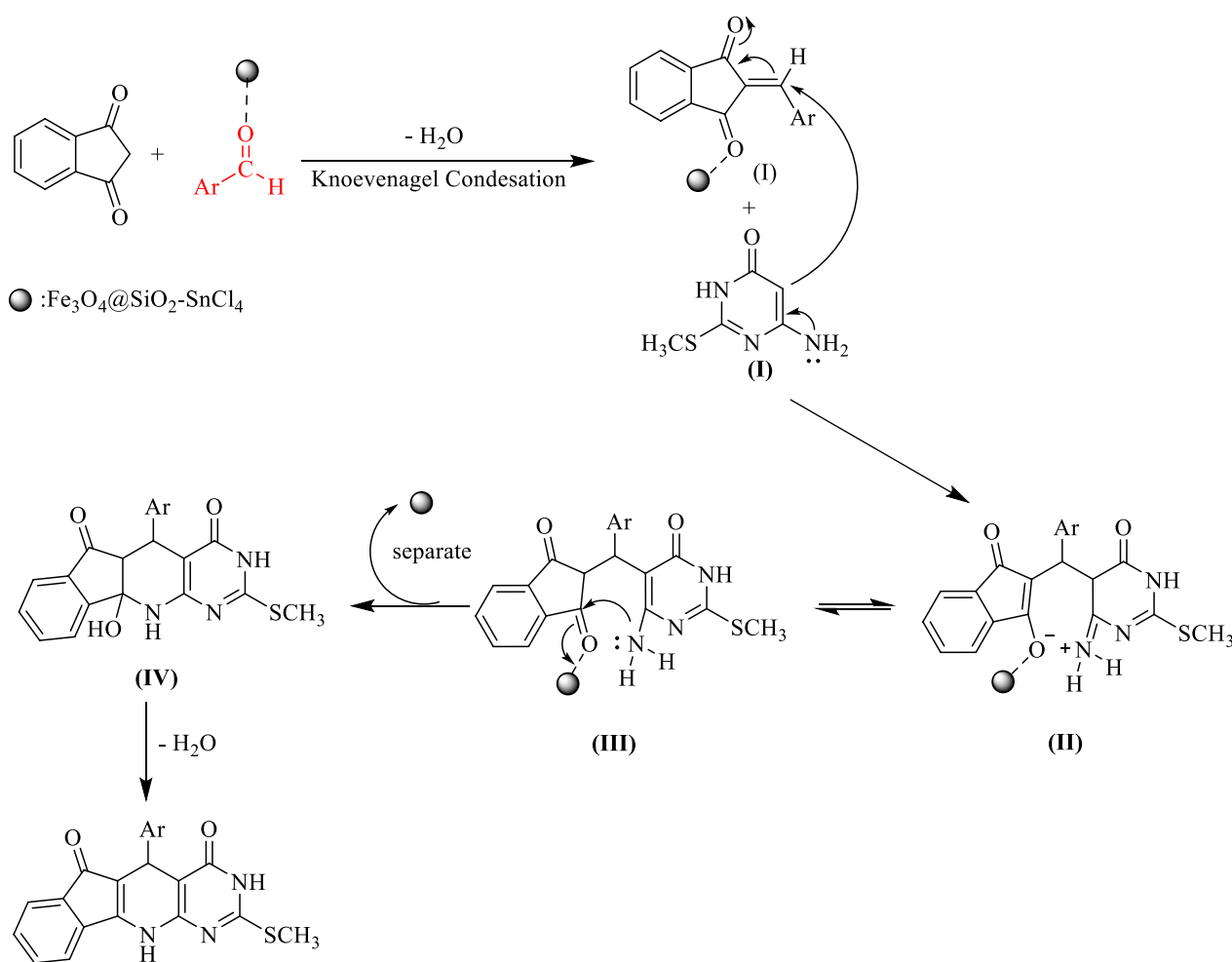


**Fig. 3** Proposed mechanism for the synthesis of indenopyrido[2,3-d]pyrimidines in the presence of  $\text{Fe}_3\text{O}_4@\text{SiO}_2\text{-SnCl}_4$

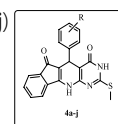
in the preparation of **4 g** as a model reaction. After completion of the reaction,  $\text{Fe}_3\text{O}_4@\text{SiO}_2\text{-SnCl}_4$  can be easily separated using an external magnet. The recovered catalyst was washed with ethanol (15 mL) and dried at room temperature without further purification for use in the next run of the current reaction under identical conditions. The results showed that after five successive runs, the catalytic activity of the catalyst was retained without significant loss of activity.

#### Cytotoxic activities

The in vitro cytotoxicity effects of indenopyrido[2,3-d]pyrimidine analogues (**4a-4j**) were assessed against three cancer cell lines including MCF-7 (breast carcinoma), A549 (lung non-small cell carcinoma), and SKOV3 (ovarian carcinoma) using the MTT assay [45, 46], and the obtained results are summarized in Table 4. Among the tested compounds, **4a** and **4f** were the most active compounds against the investigated cancer cell

lines. Compound **4f** exhibited strong anti-proliferative activity, with  $\text{IC}_{50}$  values of  $48.30 \pm 4.12$ ,  $37.90 \pm 0.73$ , and  $62.5 \pm 2.6$   $\mu\text{M}$  against A549, MCF-7, and SKOV3 cell lines, respectively. In comparison, the  $\text{IC}_{50}$  values of cisplatin were  $50.81 \pm 3.10$ ,  $61.56 \pm 0.98$  and  $43.81 \pm 3.79$   $\mu\text{M}$ , respectively. Furthermore, compounds **4b** and **4i** indicated moderate cytotoxic activity against investigated cancer cell lines.

According to the findings, the type and position of phenyl ring substitutions have a significant impact on the cytotoxic activity of these compounds. It was observed that several of the tested compounds exhibited anti-proliferative activity against the investigated cancer cell lines, while some did not demonstrate cytotoxic effects. Considering the chemical structures of the compounds and their various substitutions on the phenyl ring, revealed that the most potent compound, **4f**, contains a fluorine group in the para position of the phenyl ring. Hence, it can be concluded that the smallest and the most

**Table 4** Structures and *in vitro* cytotoxic activities of indenopyrido[16]pyrimidine derivatives (**4a-4j**)

Compound	R	IC <sub>50</sub> ± SD (μM)			
		A549	MCF7	SKOV3	MRC-5
4a	H	79.88 ± 2.81	91.72 ± 2.86	121.12 ± 11.4	> 100
4b	2-OH	193.77 ± 0.3	228.6 ± 12.97	528.88 ± 19.27	> 100
4c	2-Cl	> 1000	> 1000	> 1000	N.D
4 d	2-Br	> 1000	> 1000	> 1000	N.D
4e	2-NO <sub>2</sub>	> 1000	> 1000	> 1000	N.D
4f	4-F	48.30 ± 4.12	37.90 ± 0.73	62.5 ± 2.6	98.3 ± 3.1
4 g	4-Cl	> 1000	> 1000	> 1000	N.D
4 h	4-Br	> 1000	> 1000	> 1000	N.D
4i	2,4-di-Cl	407.76 ± 27.57	504.36 ± 23.91	424.63 ± 5.05	> 100
4j	3-OMe-4-OH	> 1000	> 1000	> 1000	N.D
Cisplatin	–	50.81 ± 3.10	61.56 ± 0.98	43.81 ± 3.79	

N.D Not Determined

electronegative halogens significantly enhance the cytotoxic effects of this class of compounds. Additionally, it was observed that removing the fluorine (compound **4a**) resulted in decreased cytotoxicity. Furthermore, the presence of a hydroxyl group in the ortho position of the phenyl ring (compound **4b**), also led to moderate cytotoxic activity. However, placing the hydroxyl group in the para position of the phenyl ring (compound **4j**) did not improve cytotoxic effects compared to the ortho position. Additional evaluations of the tested compounds indicated that a compound with two chlorine groups at positions 2 and 4 of the phenyl ring (compound **4i**) exhibited moderate cytotoxicity against A549, MCF-7, and SKOV3 cell lines. As dedicated in Table 4, all tested derivatives showed lower cytotoxic effects on the normal cell line (MRC-5) compared to other studied cancer cell lines, which revealed that they have desire selectivity between tumorigenic and non-tumorigenic cell lines. The structure activity relationship indicated that the nature and the size of substituent effect on cytotoxic potential of compounds, In para-substituted compounds, the presence of smaller substituents generally enhances the efficacy. This improvement is likely attribute to reduced steric hindrance, facilitating more effective binding or interactions. Furthermore, for ortho-substituted compounds, the presence of an -OH group appears to positively influence efficacy. This effect may be due to the formation of intramolecular hydrogen bonds and stabilizing a six-membered ring conformation. Additionally,

substituting the -OH group with chlorine or bromine moieties led to diminish the cytotoxic effects, too.

#### Docking studies

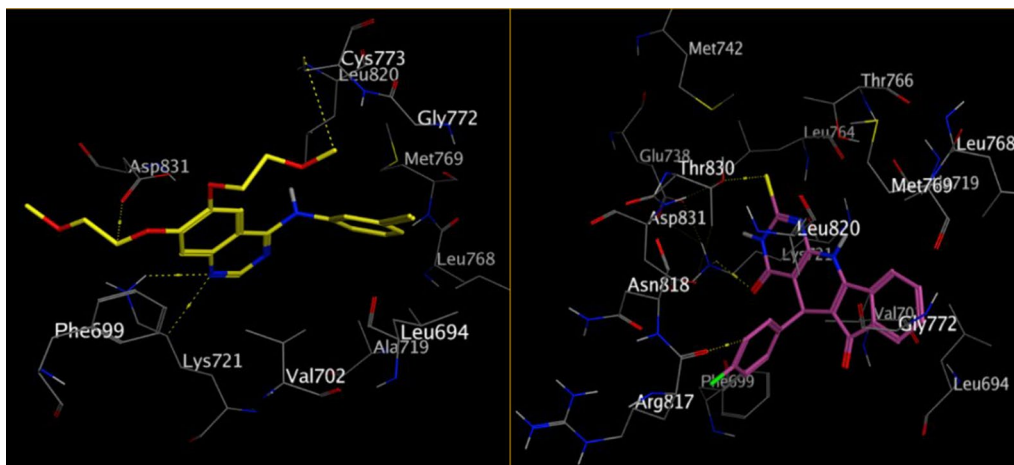
Molecular docking technique revealed the pattern of interaction between the ligand and receptor at the active site. This approach can describe the behavior of the ligand in the binding site of the target protein. The pyrido [2,3-d] pyrimidine derivatives have shown promising inhibitory activity against EGFR kinase as antitumor target [47–49], on the other hand, The MCF-7 breast cancer cell line is a well-established model for estrogen receptor alpha (ERα)-positive breast cancer, with approximately 80% of its cells expressing functional ERα. This high ERα expression makes it critical to incorporate ERα into *in silico* analyses [50]. The docking study was conducted to predict the binding modes, affinities, and orientations of the target compounds in the active sites of receptor. Table 5 summarizes the molecular docking results, including the lowest binding energy (kcal/mol) of ligand-complex.

#### Docking study on EGFR

The binding free energies of all investigated compounds were found to be more negative than the binding energy of Erlotinib, the main inhibitor of EGFR (Table 5). The highest binding energies were observed for compounds **4a** and **4f**, which also exhibited the most antitumor activity among the tested compounds. This may be attributed to their strong binding to the EGFR active site, facilitated

**Table 5** The bonding energies (Kcal/mol) of the tested compounds using AutoDock vina

Entry	4a	4b	4c	4d	4e	4f	4g	4h	4i	4j	Erlotinib	OHT
Binding energy (Kcal/mol) (1M17)	-10.5	-9.2	-9.5	-9.3	-9.6	-10.3	-9.6	-9.6	-9.7	-9.3	-7.0	--
Binding energy (Kcal/mol) (3ERT)	-7.9	-8.1	-8.3	-8.1	-8.6	-8.6	-7.5	-7.9	-8.2	-7.7	--	-7.5

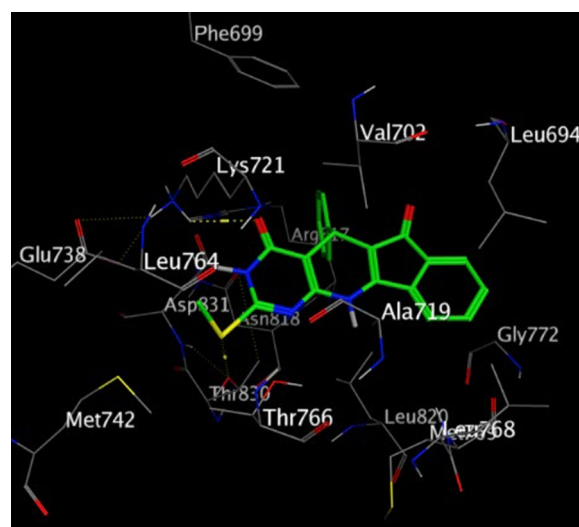
**Fig. 4** The main interaction of Erlotinib (yellow) and **4f** (pink) in the active site of EGFR (PDB ID: 1M17)

by the formation of two key hydrogen interactions. In compound **4f**, one hydrogen acceptor interaction was observed with a value of  $-1.7$  (Kcal/mol) between the carbony oxygen of the pyrimidine ring and Lys721 residue ( $3.28 \text{ \AA}$ ). The other hydrogen bond formed via an acceptor interaction between the sulfur atom in the pyrido[2,3-d] pyrimidine ring and Thr830 residue ( $3.69 \text{ \AA}$ ). The modes of interaction for compound **4f** and Erlotinib are illustrated in Fig. 4.

The binding mode of compound **4i** with EGFR implied that the hydrogen atom attached to the nitrogen of the pyrimidine ring is involved in a hydrogen donor-acceptor interaction with Asp831, with a binding energy of  $-1.1$  kcal/mol ( $2.97 \text{ \AA}$ ). Additionally, the sulfur atom of the pyrido[2,3-d] pyrimidine ring also interacted with Lys721 through a hydrogen acceptor interaction (Fig. 5).

#### Docking study on estrogen receptor alpha (ER $\alpha$ )

As shown in Tables 5, **4f** had the best binding energy,  $-8.6$  kcal/mol, as well as the reference compound, **OHT**,  $-7.5$  kcal/mol. The orientations of pyrido[1]pyrimidinone scaffold of **4f** and **4i** was displayed in Fig. 6. Docking studies indicated that two amino acid of active site of *estrogen receptor alpha*, Thr 347 and Val 534, have made key interactions through hydrogen bond interaction with

**Fig. 5** The structure of **4i** surrounded by the key residue in the active site of EGFR

methyl thio linker of pyrido[1]pyrimidinone scaffold and halogen bond donation of the fluoro atom at phenyl ring. On the other hand, **4i** interacts via pi-pi interaction between indolin ring and Leu 525.

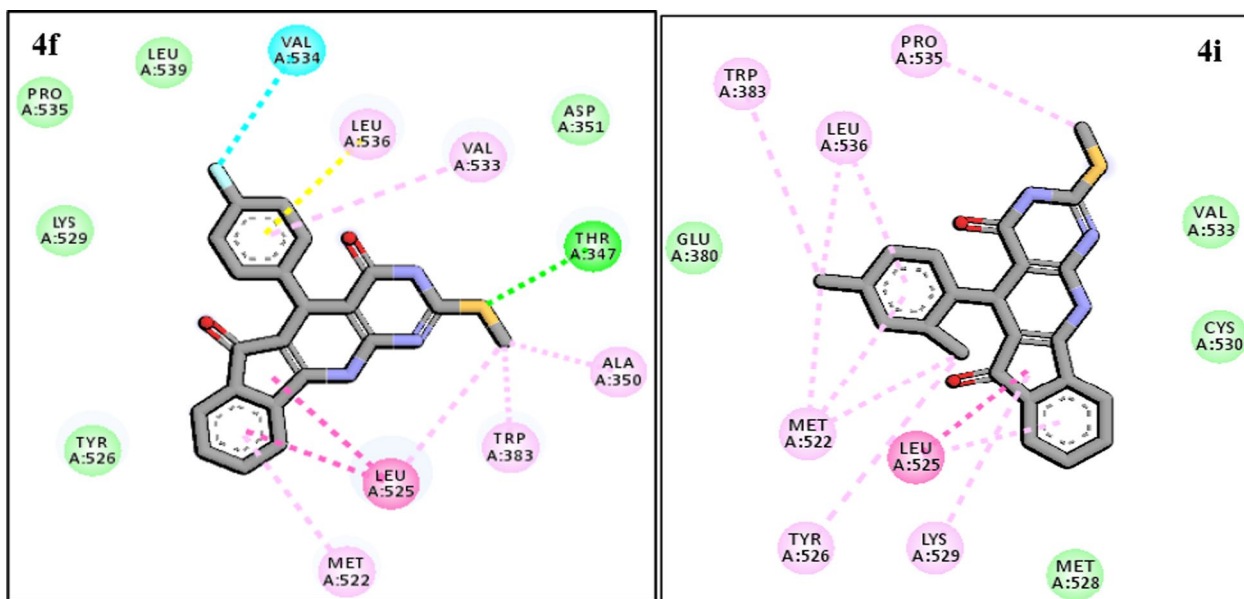


**Fig. 6** The interaction and binding mode of **4f** and **4i** in the active site of *estrogen receptor alpha* (ERA) (PDB ID: 3ERT)

#### Molecular dynamic simulation

**RMSD** The molecular dynamics simulation (MD) is commonly applied to find out the biophysical structural stability of protein structures [51–53]. The MD simulation was used to consider the dynamic behavior of the protein–ligand systems to validate the results of the molecular docking study. The RMSD of total systems were calculated using a 100-ns MD simulation for the modeled protein–ligand complex (Fig. 7). The RMSD of the system

rises sharply at the first time of the simulation and then reached a stable level from 50 ns. The RMSD plot showed that the chosen ligands in all systems exhibited consistent stability within the active site of the protein and this simulation time was sufficient enough for equilibration of the systems.

The RMSF analysis measured the fluctuations and the flexibility of amino acid residues of the protein during the molecular dynamics simulations [54]. A higher

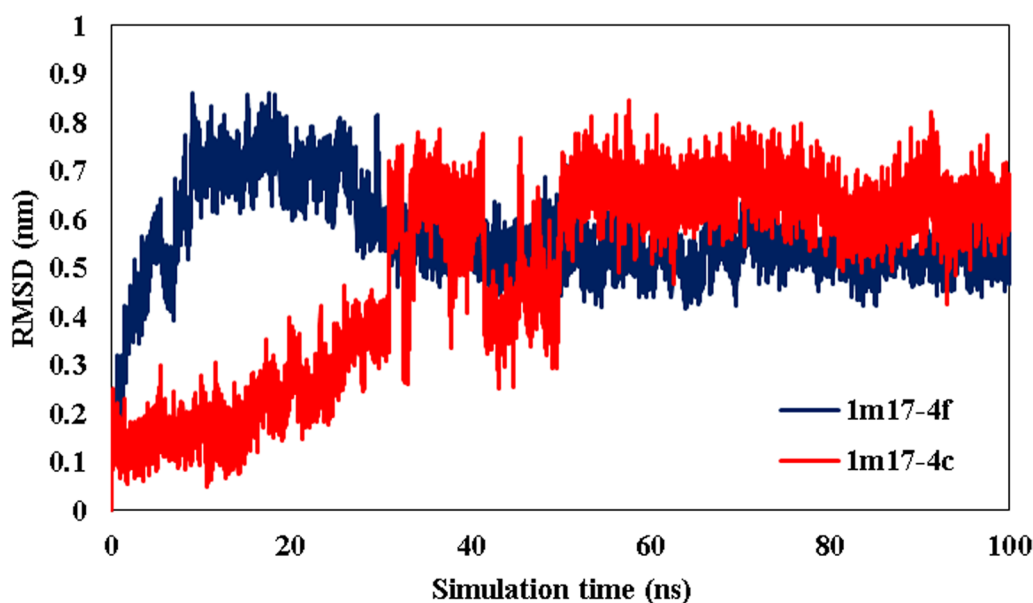


**Fig. 7** RMSD of the total system during simulation time

RMSF value shows greater flexibility and movement of the residue of protein during the simulation time, while a lower value of RMSF values indicated less conformational changes and increased stability of the protein in the complex with the ligand [55]. The RMSF data demonstrated that the fluctuations of most amino acids are between 0.2 and 0.4 nm. Two complexes displayed similar patterns. Furthermore, the RMSF plot indicated that the ligand–protein complex had no significant effect on the backbone of protein (Fig. 8).

**Radius gyration** In order to evaluate compactness of a protein, the gyration radius diagram of each complex was recorded during the simulation time. (Fig. 9) The initial value of Rg for the 4f and 4c ligands were 2.3 nm and in ranging between 2.08 nm and 2.21 nm, respectively. After 100 ns the simulation run, the Rg of the protein in complex with ligands were stable and without fluctuation. As shown in Fig. 9, the Rg of 4f-1M17 was lower than 4c-1M17, and demonstrates that more compactness of protein, more affinity of ligand in the active site protein, and stable complex. The lower values of Rg evidenced the stability the higher compactness of the protein backbone.

**Number of hydrogen bond** The number of hydrogen bonded interaction between ligand and receptor protein plays an important role to ascertain the stability of complex structure [56]. The average of number of hydrogen bonded interactions for 4f-1M17 and 4c-1M17 were observed to be 1.08 and 0.93, respectively (Fig. 10). The

number of 4f-1M17 hydrogen bonds was more, and reflecting the strong adherence between 4f in active site of protein. The obtained numbers of intermolecular hydrogen bonded interactions between ligands and 1M17 through the MD simulations run were agreed with the results in molecular docking study.

## Material and methods

### Materials and apparatus

Chemicals and solvents were purchased from Merck and Aldrich companies. FT-IR spectra were recorded as KBr pellet on a Bruker, Equinox 55 spectrometer.  $^1\text{H}$  NMR and  $^{13}\text{C}$ -NMR was recorded on a 400 MHz Bruker DRX-400 in DMSO- $d_6$  as solvent and TMS as an internal standard. Melting points were obtained with a Buchi melting point B-540 B.V.CHI apparatus. Ultrasonic irradiations was done using Elmasonic S 40H ultrasonic cleaning.

### Cytotoxicity activity

#### Cell line and cell culture

Three human cancer cell lines, MCF-7 (breast carcinoma), A549 (lung non-small cell carcinoma), SKOV3 (ovarian carcinoma) and normal lung cell (MRC-5) were purchased from National Cell Bank of Iran (NCBI, Pasteur Institute, Tehran, Iran). The cells were cultured in complete culture media containing RPMI 1640, 10% fetal bovine serum (FBS) and 1% penicillin–streptomycin (all from Gibco, USA) at 37 °C in a humidified  $\text{CO}_2$  incubator.

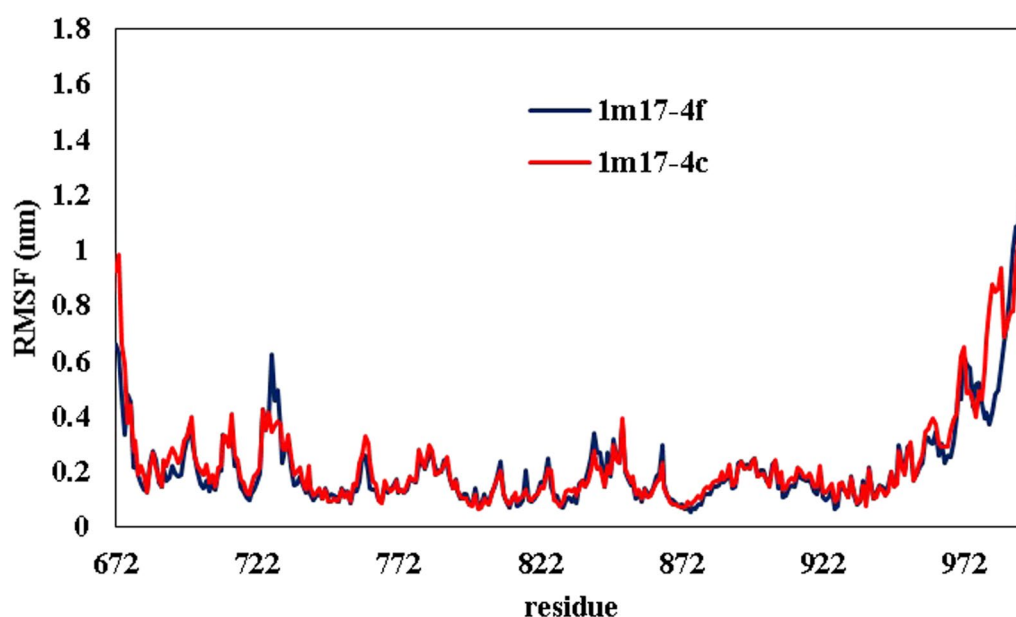


**Fig. 8** RMSF analysis of the protein backbone atoms of the 1M17 in complexes with 4f and 4c ligands

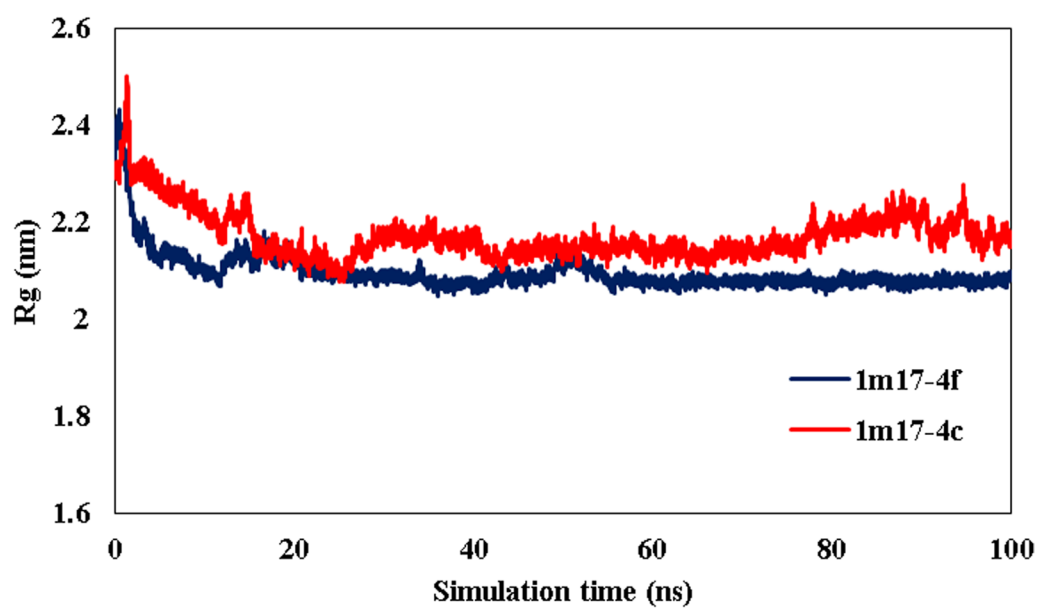


**Fig. 9** Radius of gyration during the simulation process

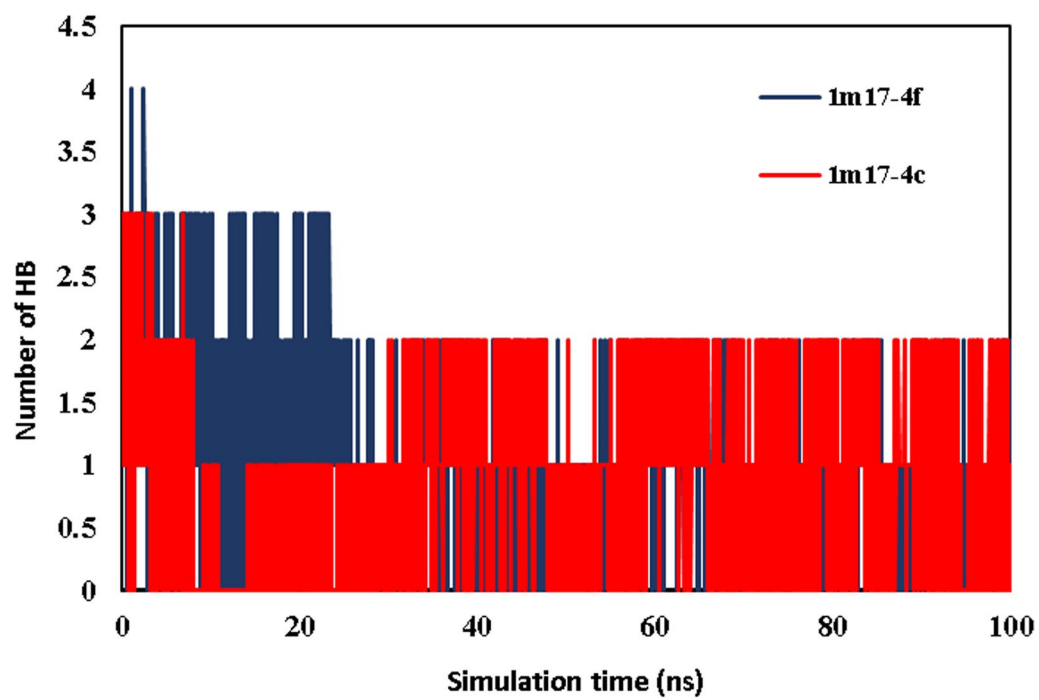


**Fig. 10** Number of hydrogen bonds between ligands and protein through simulation time

### MTT assay

To determine the cytotoxic activities of ten indenopyrido[2,3-d]pyrimidine derivatives, a standard MTT assay was used, as previously reported [57, 58]. Briefly, the cells were seeded in 96-well microplates at a density of  $1 \times 10^4$  cells per well in 100  $\mu$ L of complete culture medium. After 24 h, the cells were treated with different concentrations of the compounds (1–1000  $\mu$ M) in triplicate manner for 72 h. The final DMSO concentration maintained at less than 0.1%. DMEM/Ham's F12 (Bio Idea, Iran) was applied for normal cell line (MRC-5). The media were then completely removed and replaced with 150  $\mu$ L of RPMI 1640 containing 0.5 mg/mL MTT solution. The plate was then returned to the incubator for an additional 3 h until intracellular purple formazan crystals appeared. The media were then discarded, and 150  $\mu$ L DMSO was added, followed by incubation at 37 °C in the dark for 30 min to dissolve the crystals. The absorbance of each well was then measured at 490 nm.

### Data analysis

To estimate and analyze the data, Excel 2013 and CurveExpert 1.4 were used. The following formula was applied to measure the percentage of inhibitory effect of each compound:

$$IC_{50} = 100 - \left[ \frac{(OD_{\text{test}} - OD_{\text{blank}})}{(OD_{\text{negative}})} \times 100 \right]$$

A plot of the inhibition concentration versus concentration was created and the Inhibition Concentration 50 ( $IC_{50}$ ), demonstrating the 50% growth inhibition of the cells, was obtained. Data are reported as mean  $\pm$  SD in Table 1.

### Docking procedure

The docking simulation carried out by an in house batch script (DOCK-FACE) for automatic running of Auto vina [59] in a parallel mode, using all system resources as described in our recent studies [60, 61]. Firstly, PDB ligand structures were prepared using Hyper Chem Professional Version 8 (Hypercube Inc., Gainesville, FL, USA). They were then geometrically optimized by Molecular Mechanics (MM<sup>+</sup>) following semi empirical AM1 method. To obtain PDBQT format for each ligand,gasteiger charges were implemented, non-polar hydrogen of compounds were merged and rotatable bonds were assigned by MGL tools 1.5.6 [62]. For preparing receptor structures, the 3D crystal structure of EGFR (PDB ID: 1M17) was retrieved from Protein Data Bank (PDB data base; <http://www.rcsb.org>) [63]. In each structure, all water molecules and co-crystal ligand were removed and missing hydrogens were added. The PDBs were then

checked for missing atoms with MODELLER 9.17 [37]. For Lamarckian GA method, the prepared ligands were given to 100 independent genetic algorithm (GA) runs, 150 population size, maximum number of 2,500,000 energy evaluations, gene mutation rate of 0.02 and 27,000 maximum generations were used. A grid box of 70.70  $\times$  70.70 points in x, y, and z directions was built and centered on the ligand. Number of points in x, y and z was 20.14, and 0.3, and 52.2. For internal validation, co-crystal ligand for each receptor individually, was excluded and treated the same as examined ligand. All the docking procedures were done on validated procedure with a root mean square deviation (RMSD) value below of 2 Å. All interactions were visualized and evaluated on the basis of docking results by VMD software [59].

### Molecular dynamics simulation

Analyzing the dynamic nature of ligand–protein complex was done using GROMACS software for 100 ns molecular dynamics (MD) simulation. The simulations were conducted using an AMBER force field. Tipp3 water molecules were added to the simulation box. Periodic boundary conditions (PBC) were applied to all three directions of the system. Initially, for energy minimization, the steepest descent algorithm was applied. Then, the system was equilibrated by NVT and NPT ensembles respectively. All parameters for MD simulation were set according to previous study [64]. The analysis of Root Mean Square Deviation (RMSD), Root Mean Square Fluctuation (RMSF), the Radius of gyration (Rg), and the number of hydrogen bonds (HB) were analyzed through the MD trajectories.

### Conclusion

In summary, we have showed for the first time that  $Fe_3O_4@SiO_2-SnCl_4$  is an effective heterogeneous catalyst for the one-pot synthesis of indenopyrido[2,3-d]pyrimidine derivatives from 6-amino-2-(methylthio)pyrimidin-4(3H)-one, 1,3-indanedione and aryl aldehydes under reflux and ultrasound irradiation conditions in water. The mild reaction conditions, green and cost-effective catalyst, excellent yields, easy work-up procedures, which avoid the use of large volumes of hazardous organic solvents, make this approach a valuable alternative to previously reported procedures. Compared to non-magnetic nanoparticle catalytic systems, the present protocol combines the advantages of solid Lewis acids and magnetic nanoparticles, offering significant potential for the rapid synthesis of indenopyrido[2,3-d]pyrimidine derivatives. The cytotoxicity results showed the acceptable effect of

some of these compounds, especially the compound 4F. Additionally, docking outputs showed significant hydrogen bonding interactions, especially with Lys 721 and Thr 830 in active site of EGFR kinase that are necessary for the ligand's inhibitory effectiveness. The molecular dynamic simulation was applied to investigate the dynamic behavior of the complexes and confirm the results of the molecular docking.

## Supplementary Information

The online version contains supplementary material available at <https://doi.org/10.1186/s13065-025-01489-z>.

Additional file 1

## Acknowledgements

Not Applicable

## Author contributions

L.E. prepare the manuscript and performed docking study. L.B. wrote the simulation section. A.M.A. supervised the study and contribute to revise the manuscript. S. S. contributed to the synthesis of compounds. B.B.F.M. synthesized of compounds. Z. F. contributed to the preparation of the manuscript. S.Kh. performed the biological assay. L.Z. supervised the biological tests. S. Kh. edit the manuscript and supervised the study. All authors read and approved the final manuscript.

## Funding

Financial assistance from the Shiraz University of Medical Sciences by way of grant number 10685 is gratefully acknowledged.

## Availability of data and materials

The data sets used and analyzed during the current study are available from the corresponding author on reasonable request. We have presented all data in the form of Tables and Figure. The PDB code (1M17) was retrieved from protein data bank ([www.rcsb.org](http://www.rcsb.org)). <https://www.rcsb.org/structure/1M17>.

## Declarations

### Ethics approval and consent to participate

Not applicable.

### Consent for publication

Not applicable.

### Competing interests

The authors declare no competing interests.

Received: 10 January 2025 Accepted: 23 April 2025

Published online: 16 May 2025

## References

- Zheng L-W, et al. Synthesis of novel oxime-containing pyrazole derivatives and discovery of regulators for apoptosis and autophagy in A549 lung cancer cells. *Bioorg Med Chem Lett*. 2010;20(16):4766–70.
- Patrick GL. An introduction to medicinal chemistry. Oxford: Oxford University Press; 2013.
- Kang L, et al. Structure–activity relationship investigation of coumarin–chalcone hybrids with diverse side-chains as acetylcholinesterase and butyrylcholinesterase inhibitors. *Mol Diversity*. 2018;22:893–906.
- DeGraw JI, et al. Antimicrobial activity of 8-deazafoolic acid. *J Med Chem*. 1974;17(4):470–1.
- Matsumoto J, Minami S. Pyrido [2, 3-d] pyrimidine antibacterial agents 3 8-alkyl-and 8-vinyl-5, 8-dihydro-5-oxo-2-(1-piperazinyl) pyrido [2, 3-d] pyrimidine-6-carboxylic acids and their derivatives. *J Med Chem*. 1975;18(1):74–9.
- Oakes V, Rydon H. 853 Polyanaphthalenes Part IV Further derivatives of 1: 3: 5-and 1: 3: 8-triazanaphthalene. *J Chem Soc (Resumed)*. 1956. <https://doi.org/10.1039/jr9560004433>.
- Suzuki N. Synthesis of antimicrobial agents V Synthesis and antimicrobial activities of some heterocyclic condensed 1, 8-naphthyridine derivatives. *Chem Pharmaceut Bull*. 1980;28(3):761–8.
- Font M, et al. New insights into the structural requirements for pro-apoptotic agents based on 2, 4-diaminoquinazoline, 2, 4-diaminopyrido [2, 3-d] pyrimidine and 2, 4-diaminopyrimidine derivatives. *Eur J Med Chem*. 2011;46(9):3887–99.
- Broom AD, Shim JL, Anderson GL. Pyrido [2, 3-d] pyrimidines IV Synthetic studies leading to various oxopyrido [2, 3-d] pyrimidines. *J Organic Chem*. 1976;41(7):1095–9.
- Grivsky EM, et al. Synthesis and antitumor activity of 2, 4-diamino-6-(2, 5-dimethoxybenzyl)-5-methylpyrido [2, 3-d] pyrimidine. *J Med Chem*. 1980;23(3):327–9.
- Agarwal A, et al. Dihydropyrido [2, 3-d] pyrimidines as a new class of antileishmanial agents. *Bioorg Med Chem*. 2005;13(24):6678–84.
- Bouzard D. Antibiotics and antiviral compounds. Weinheim: VCH; 1993.
- Pastor A, et al. Synthesis and structure of new pyrido [2, 3-d] pyrimidine derivatives with calcium channel antagonist activity. *Tetrahedron*. 1994;50(27):8085–98.
- El-Gazzar A-RB, Hafez HN. Synthesis of 4-substituted pyrido [2, 3-d] pyrimidin-4 (1H)-one as analgesic and anti-inflammatory agents. *Bioorg Med Chem Lett*. 2009;19(13):3392–7.
- Gangjee A, Adair O, Queener SF. Pneumocystis carinii and Toxoplasma gondii Dihydrofolate Reductase Inhibitors and Antitumor Agents: Synthesis and Biological Activities of 2, 4-Diamino-5-methyl-6-[(monosubstituted anilino) methyl]-pyrido [2, 3-d] pyrimidines. *J Med Chem*. 1999;42(13):2447–55.
- Gangjee A, et al. 2, 4-Diamino-5-deaza-6-substituted pyrido [2, 3-d] pyrimidine antifolates as potent and selective nonclassical inhibitors of dihydrofolate reductases. *J Med Chem*. 1996;39(7):1438–46.
- Hamby JM, et al. Structure–activity relationships for a novel series of pyrido [2, 3-d] pyrimidine tyrosine kinase inhibitors. *J Med Chem*. 1997;40(15):2296–303.
- Ghorab MM, Alsaïd MS. Synthesis of some tricyclic indeno [1, 2-d] pyrimidine derivatives as a new class of anti-breast cancer agents. *Biomed Res*. 2015;26(3):420–5.
- Manpadi M, et al. Three-component synthesis and anticancer evaluation of polycyclic indenopyridines lead to the discovery of a novel indenoheterocycle with potent apoptosis inducing properties. *Org Biomol Chem*. 2007;5(23):3865–72.
- Ghahremanzadeh R, et al. One-Pot, Pseudo four-component synthesis of a spiro [diindeno [1, 2-b: 2', 1'-e] pyridine-11, 3'-indoline]-trione library. *J Comb Chem*. 2010;12(1):191–4.
- Ghorab MM, et al. Novel antitumor and radioprotective sulfonamides containing pyrrolo [2, 3-d] pyrimidines. *Arzneimittelforschung*. 2006;56(06):405–13.
- Jing R, Jiang Z, Tang X. Advances in millimeter-wave treatment and its biological effects development. *Int J Mol Sci*. 2024;25(16):8638.
- Zhang Y-W, et al. Effect of oridonin on cytochrome P450 expression and activities in HepaRG cell. *Pharmacology*. 2018;101(5–6):246–54.
- Bazgir A, et al. A clean, three-component and one-pot cyclo-condensation to pyrimidine-fused heterocycles. *C R Chim*. 2009;12(12):1287–95.
- Hassan NA, et al. Three-component, one-pot synthesis of pyrimido [4, 5-b]-quinoline and pyrido [2, 3-d] pyrimidine derivatives. *J Heterocycl Chem*. 2007;44(4):775–82.
- Huang Z, et al. Efficient one-pot three-component synthesis of fused pyridine derivatives in ionic liquid. *ACS Comb Sci*. 2011;13(1):45–9.
- Shi F, et al. Substrate-controlled chemoselective synthesis and potent cytotoxic activity of novel 5, 6, 7-triarylpyrido [2, 3-d] pyrimidin-4-one derivatives. *Bioorg Med Chem Lett*. 2011;21(5):1554–8.

28. Tu S, et al. An efficient synthesis of pyrido [2, 3-d] pyrimidine derivatives and related compounds under ultrasound irradiation without catalyst. *Ultrason Sonochem.* 2008;15(3):217–21.
29. Tu S, et al. New potential inhibitors of cyclin-dependent kinase 4: design and synthesis of pyrido [2, 3-d] pyrimidine derivatives under microwave irradiation. *Bioorg Med Chem Lett.* 2006;16(13):3578–81.
30. Li R, et al. Clinical features, treatment, and prognosis of SGLT2 inhibitors induced acute pancreatitis. *Expert Opin Drug Safety.* 2024. <https://doi.org/10.1080/14740338.2024.2396387>.
31. Gholami A, Mokhtary M, Nikpassand M. Glycolic acid-supported cobalt ferrite-catalyzed one-pot synthesis of pyrimido [4, 5-b] quinoline and indenopyrido [2, 3-d] pyrimidine derivatives. *Appl Organomet Chem.* 2020;34(12): e6007.
32. Safajoo N, Mirjalili BBF, Bamoniri A. A facile and clean synthesis of indenopyrido [2, 3-d] pyrimidines in the presence of Fe<sub>3</sub>O<sub>4</sub>@NCs/Cu (II) as bio-based magnetic nano-catalyst. *Polycyclic Aromat Compd.* 2021;41(6):1241–8.
33. Cheng Y, et al. The Investigation of Nfkb inhibitors to block cell proliferation in OSCC cells lines. *Curr Med Chem.* 2024. <https://doi.org/10.2174/0109298673309489240816063313>.
34. Bamoniri A, Fouladgar S. SnCl<sub>4</sub>-functionalized nano-Fe<sub>3</sub>O<sub>4</sub> encapsulated-silica particles as a novel heterogeneous solid acid for the synthesis of 1, 4-dihydropyridine derivatives. *RSC Adv.* 2015;5(96):78483–90.
35. Bamoniri A, Mirjalili BBF, Fouladgar S. Fe<sub>3</sub>O<sub>4</sub>@SiO<sub>2</sub>-SnCl<sub>4</sub>: an efficient catalyst for the synthesis of xanthene derivatives under ultrasonic irradiation. *Polycyclic Aromat Compd.* 2017;37(5):345–61.
36. Wang K, et al. Inhibition of inflammation by berberine: molecular mechanism and network pharmacology analysis. *Phytomedicine.* 2024;128: 155258.
37. Akrami H, et al. 9H-carbazole derivatives containing the N-Benzyl-1, 2, 3-triazole moiety as new acetylcholinesterase inhibitors. *Arch Pharm.* 2015;348(5):366–74.
38. Akrami H, et al. Indolinone-based acetylcholinesterase inhibitors: synthesis, biological activity and molecular modeling. *Eur J Med Chem.* 2014;84:375–81.
39. Mirjalili BF, et al. Synthesis, antifungal activity and docking study of 2-amino-4H-benzochromene-3-carbonitrile derivatives. *J Mol Struct.* 2016;1116:102–8.
40. Zamani L, Mirjalili BBF. Synthesis and characterization of tetraarylporphyrins in the presence of nano-TiCl<sub>4</sub>·SiO<sub>2</sub>. *Chem Heterocycl Compd.* 2015;51:578–81.
41. Zamani L, et al. Synthesis of benzimidazoles in the presence of nano-TiCl<sub>4</sub>·SiO<sub>2</sub> as antifungal agents and tautomerism theoretical study of some products. *Synthesis.* 2014;62:3.
42. Azad S, Mirjalili BBF. Fe<sub>3</sub>O<sub>4</sub>@ nano-cellulose/TiCl<sub>4</sub>: a bio-based and magnetically recoverable nano-catalyst for the synthesis of pyrimido [2, 1-b] benzothiazole derivatives. *RSC Adv.* 2016;6(99):96928–34.
43. Bamoniri A, Moshtael-Arani N. Nano-Fe<sub>3</sub>O<sub>4</sub> encapsulated-silica supported boron trifluoride as a novel heterogeneous solid acid for solvent-free synthesis of arylazo-1-naphthol derivatives. *RSC Adv.* 2015;5(22):16911–20.
44. Mirjalili BBF, Bamoniri A, Azad S. Synthesis of 2, 3-dihydroquinazolin-4 (1 H)-ones catalyzed by nano-Fe<sub>3</sub>O<sub>4</sub>/TiCl<sub>4</sub>/cellulose as a bio-based magnetic catalyst. *J Iran Chem Soc.* 2017;14:47–55.
45. Zhao L, et al. Aminoselenation and dehydroaromatization of cyclohexanones with anilines and diselenides. *Org Lett.* 2024;26(22):4835–9.
46. Wang Y, et al. Synthesis of 4 H-Pyrazolo [3, 4-d] pyrimidin-4-one hydrazine derivatives as a potential inhibitor for the self-assembly of TMV particles. *J Agric Food Chem.* 2024;72(6):2879–87.
47. Elzahabi HS, et al. Anticancer evaluation and molecular modeling of multi-targeted kinase inhibitors based pyrido [2, 3-d] pyrimidine scaffold. *J Enzyme Inhib Med Chem.* 2018;33(1):546–57.
48. Muhammad Z, et al. Synthesis, antitumor evaluation and molecular docking of new morpholine based heterocycles. *Molecules.* 2017;22(7):1211.
49. Zeng X, et al. The miR-665/SOST axis regulates the phenotypes of bone marrow mesenchymal stem cells and osteoporotic symptoms in female mice. *Am J Pathol.* 2024;194(11):2059–75.
50. Horwitz K, Costlow M, McGuire WL. MCF-7: a human breast cancer cell line with estrogen, androgen, progesterone, and glucocorticoid receptors. *Steroids.* 1975;26(6):785–95.
51. Paul SK, et al. Molecular modeling, molecular dynamics simulation, and essential dynamics analysis of grancalcin: An upregulated biomarker in experimental autoimmune encephalomyelitis mice. *Heliyon.* 2022. <https://doi.org/10.1016/j.heliyon.2022.e11232>.
52. Sun D-Y, et al. Unlocking the full potential of memory T cells in adoptive T cell therapy for hematologic malignancies. *Int Immunopharmacol.* 2025;144: 113392.
53. Wang L, et al. Research progress on antioxidants and protein aggregation inhibitors in cataract prevention and therapy. *Mol Med Rep.* 2024;31(1):22.
54. Zare F, et al. A combination of virtual screening, molecular dynamics simulation, MM/PBSA, ADMET, and DFT calculations to identify a potential DPP4 inhibitor. *Sci Rep.* 2024;14(1):7749.
55. Bagewadi S, Veerashetty S. Fine-grained textural detail enhancement: concatenating convolutional neural network features with adaptive fuzzy logic. *SIVIP.* 2024;18(5):4615–26.
56. Yadav P, Rana M, Chowdhury P. DFT and MD simulation investigation of favipiravir as an emerging antiviral option against viral protease (3CLpro) of SARS-CoV-2. *J Mol Struct.* 2021;1246: 131253.
57. Faghiz Z, et al. Palladium (II) complexes based on Schiff base ligands derived from ortho-vanillin; synthesis, characterization and cytotoxic studies. *Inorg Chim Acta.* 2018;471:404–12.
58. Faghiz Z, et al. Synthesis of some novel dibromo-2-arylquinazolinone derivatives as cytotoxic agents. *Res Pharmaceut Sci.* 2019;14(2):115–21.
59. Humphrey W, Dalke A, Schulten K. VMD: visual molecular dynamics. *J Mol Graph.* 1996;14(1):33–8.
60. Fereidoonzhad M, et al. A comparative docking studies of dichloroacetate analogues on four isozymes of pyruvate dehydrogenase kinase in humans. *Dent.* 2016;1(4):5.
61. Mojaddami A, et al. Binding mode of triazole derivatives as aromatase inhibitors based on docking, protein ligand interaction fingerprinting, and molecular dynamics simulation studies. *Res Pharmaceut Sci.* 2017;12(1):21.
62. Morris GM, Huey R, Olson AJ. Using autodock for ligand-receptor docking. *Curr Protoc Bioinf.* 2008;24(1):814.
63. Rahmangebadi N, Khabnadideh S, Yavari I. Synthesis, docking, and cytotoxic activities of novel 2-aryl-4-(arylamino) quinazolines. *Monatshefte für Chemie-Chemical Monthly.* 2018;149(11):2085–92.
64. Baziar L, et al. Design, synthesis, biological evaluation and computational studies of 4-Aminopiperidine-3, 4-dihydroquinazolinone-2-uracil derivatives as promising antidiabetic agents. *Sci Rep.* 2024;14(1):26538.

## Publisher's Note

Springer Nature remains neutral with regard to jurisdictional claims in published maps and institutional affiliations.